ELSEVIER

Journal of Power Sources 81–82 (1999) 607–611

JOURNAL OF POWER SOURCES

www.elsevier.com/locate/jpowsour

Electrochemical behaviour of $LiMn_2O_4$–PPy composite cathodes in the 4-V region

A. Du Pasquier [a,*], F. Orsini, A.S. Gozdz [b], J.-M. Tarascon [a,b]

[a] *Laboratoire de Réactivité et de Chimie des solides, URA CNRS 1211, Université de Picardie Jules Verne, 33 Rue Saint-Leu, 80039 Amiens Cedex, France*

[b] *Bell Communications Research, Red Bank, NJ 07701-7040, USA*

Abstract

Core-shell type particles were prepared by reaction of $LiMn_2O_4$ powders in an aqueous solution of pyrrole and paratoluene sulfonic acid. Thermogravimetric analysis and X-ray diffraction studies of these organic–inorganic hybrid particles demonstrated that the polymerization of pyrrole was accompanied by delithiation of the starting spinel, manganese dissolution and creation of electrochemically inactive λ-MnO_2. This mechanism of polymerization was confirmed by changing the experimental conditions, e.g., starting from λ-MnO_2 powders and using H_2O–lithium paratoluene sulfonate medium. The protective effect of PPy coating on the cyclability at 55°C of these particles was studied in order to solve the well-known problem of capacity fading and self-discharge at elevated temperature of the $LiMn_2O_4$ spinels.

Keywords: $LiMn_2O_4$; Polypyrrole; Cyclability; Composite cathode

1. Introduction

The $LiMn_2O_4$/C system has demonstrated good feasibility for Li-ion batteries [1]. However, this system suffers from significant capacity fading and self-discharge at elevated temperatures. These problems originate at the cathode and are associated with Mn^{2+} dissolution [2]. Several improvements of the spinel were made by Bellcore's researchers by controlling the specific area, the Li stoichiometry and the annealing temperature [3]. However these problems still persist, and a significant effort is devoted worldwide to understand the mechanism(s) of the capacity fading [4,5]. Two major paths to improvement may be pointed out: structure modifications such as Co-doping [6] or replacement of oxygen by fluorine [7] and surface modifications by Mn^{2+} getters such as acetyl-acetone [8]. The approach described in this paper belongs to the second category and consists in coating the surface of spinel particles with an electronically conductive polymer, e.g., polypyrrole.

Gemeay et al. [9] described the preparation of such composites and demonstrated that they improved the utilisation of $LiMn_2O_4$ at the 3-V plateau. They reported that the presence of an acidic medium was necessary to have polymerization of the monomer at the surface of $LiMn_2O_4$ by building up negative charges that compensate those of the positively charged PPy [10]. They did not investigate the effect of such a coating on the cyclability of the 4-V plateau, the object of the present paper.

2. Experimental

$Li_{1.05}Mn_{1.95}O_4$ powder (0.8 $m^2\ g^{-1}$ BET surface area, home-made) and pyrrole (Aldrich, distilled under atmospheric pressure) were used as starting materials. The polymerization solution consisted of 200 ml of a 1 M paratoluene sulfonic acid (PTSA) aqueous solution, because of the good electrochemical stability of tosylate-doped PPy [11]. The suspension of $LiMn_2O_4$ and pyrrole was gently stirred for 5 min under atmospheric atmosphere. The mixture obtained was filtered in a Büchner funnel and washed several times with deionized water. The black powder resulting from this treatment was dried at 50°C under vacuum for 12 h. The quantities of pyrrole used were 0.1, 0.05, 0.025, 0.0125 and 0.0062 ml per gram of spinel (series A). This series was duplicated, with the exception that pyrrole was introduced first, and no stirring was used (series B). A variation of these conditions (series

* Corresponding author

0378-7753/99/$ - see front matter
PII: S0378-7753(99)00230-X

C) consisted in using H_2O–lithium paratoluene sulfonate medium and starting from the delithiated λ-Mn_2O_4 phase, chemically obtained by the acid leaching technique recognized by Hunter [12]. Samples will be named #0.1A to #0.1C, with the number referring to the amount of pyrrole and the letter referring to the series. Electrochemical cycling tests were carried out in Swagelok™ cells using a Whatman glass fiber separator and a Li metal counterelectrode. Battery-grade electrolyte stable up to 5 V vs. Li + , Li (1 M $LiPF_6$ in 2:1 v/v EC-DMC) [13] from Merck was used as received. Cathodes were typically cast from a slurry containing 65 w% $LiMn_2O_4$–PPy powder, 6.5 w% SP carbon black (MMM SA Carbon), 18.5 w% DBP (dibutyl phthalate) plasticizer and 10 w% PVDF-HFP Kynar FLEX 2801 binder (Elf-Atochem America) in acetone, according to Plion™ Bellcore's process [14]. The DBP plasticizer was extracted with diethyl ether, leaving a microporous electrode. The extracted cathodes were discs of 1.13 cm^2 area containing 20 to 30 mg of active material. They were galvanostatically cycled at various rates between 3 and 4.5 V with a Mac-Pile battery cycler (Bio-Logic) in a oven thermostated at 55°C.

3. Results and discussion

3.1. Infrared spectroscopy

FT-IR spectra of the composites were compared to the one of pure PPy prepared by oxidation of pyrrole with ferric tosylate in water. The same peaks were observed as is displayed in Table 1, which proved the presence of PPy in the $LiMn_2O_4$ powder. However, some differences were observed in the spectra (Fig. 1). In particular, the I_{1542}/I_{1443} ratios are higher for coated PPy than for pure PPy. Liang et al. [15] showed that this ratio is inversely proportional to the conjugation length in PPy's. This implies that PPy's studied in this work are less conductive than pure PPy.

3.2. Thermogravimetric analysis

$LiMn_2O_4$–PPy hybrid particle composition was also studied by TGA. Typical TGA traces of pure PPy and hybrid particles recorded at a heating rate of 5°C min^{-1} from 25 to 800°C are shown (Fig. 2). Three plateaus may be identified as evidenced by the derivative curve of the TGA signal. Below 500°C are the losses attributed to the degradation of all organic species covering the particles, e.g., polypyrrole. Thus, knowing that the burning of pure PPy results in a 100% weight loss, the weight fraction of polypyrrole is determined at the position of the second plateau (400°C). In the series B, the losses at mid-temperature (350–500°C) have decreased, which suggests that without stirring, a lower amount of polypyrrole is formed. Oxygen losses occur between 400 and 600°C, they are attributed to the formation of Mn_2O_3 [16] according to Eq. (1):

$$2\lambda\text{-}MnO_2 \rightarrow Mn_2O_3 + 1/2O_2 \quad (1)$$

Since this reaction produces 9 wt.% O_2 loss from λ-MnO_2, it is possible to determine the amount of λ-MnO_2 present in the hybrid material. The derivative TGA curves indicate that the ratio of PPy to λ-MnO_2 is not constant in the samples (cf. Fig. 3).

The main result observed is that the weight fraction of polypyrrole increased continuously as increasing the amount of pyrrole in the polymerization bath, whereas the MnO_2 content passed through a maximum and decreased at higher pyrrole contents. We explain this by the coexistence of two competitive reactions during the course of

Table 1
FT-IR peak frequencies of pure PPy and $LiMn_2O_4$ PPy composites and their peak assignments

Peak frequencies (cm^{-1})	Peak assignments
1542	C=C backbone stretching
1443	C–C ring stretching
1304	C–N ring stretching
1150	C–H in plane deformation
1031	N–H in plane deformation
623, 534	Mn–O bonds

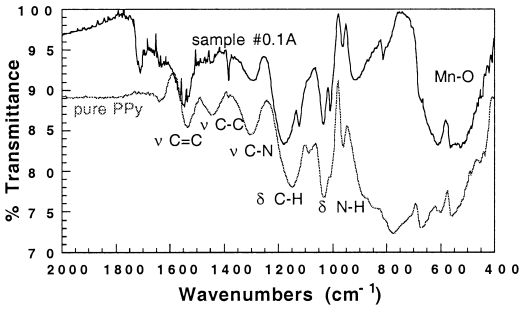

Fig. 1. FT-IR spectra of pure polypyrrole and polypyrrole coated on $LiMn_2O_4$.

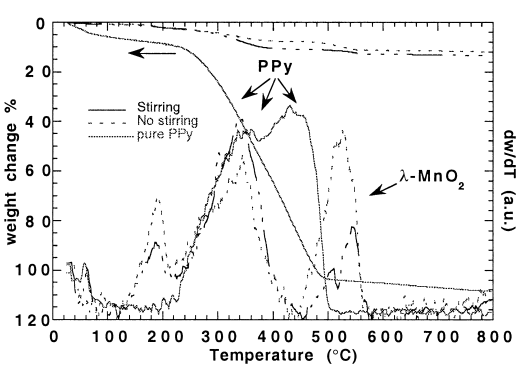

Fig. 2. TGA traces and their derivatives of pure polypyrrole and $LiMn_2O_4$–polypyrrole materials prepared with or without stirring.

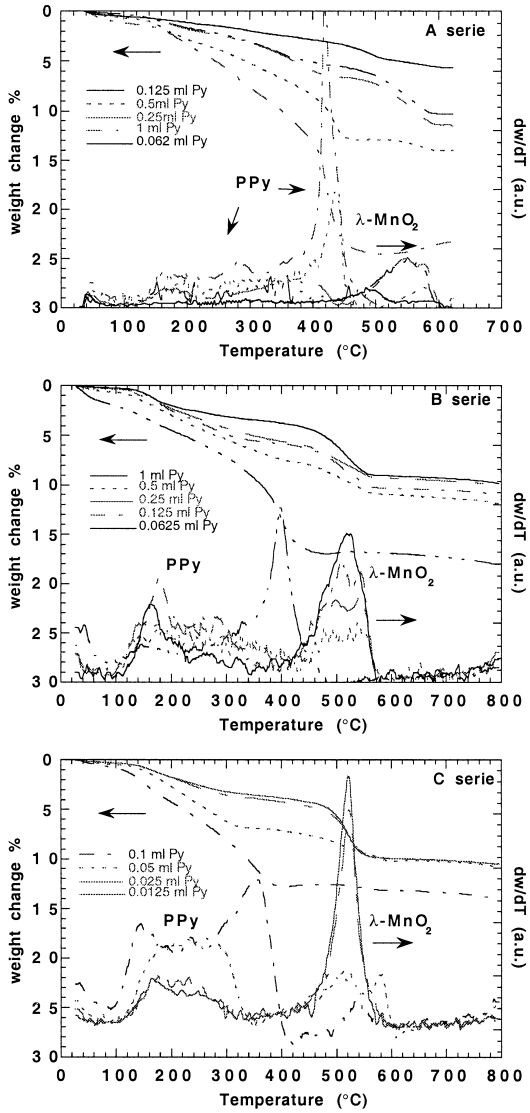

Fig. 3. TGA traces and their derivatives of all the $LiMn_2O_4$–PPy samples from series A, B and C.

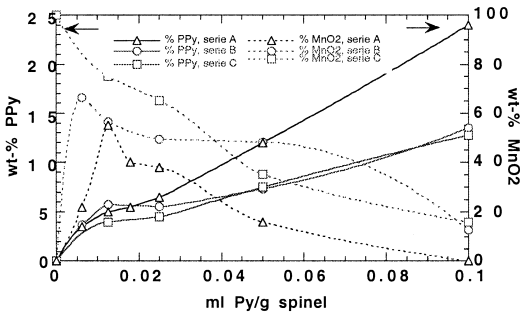

Fig. 4. PPy and λ-MnO_2 contents from TGA traces as a function of initial amount of Py used for series A, B and C.

polymerization: dismutation of $LiMn_2O_4$ in acidic medium, $2Mn^{+3} \rightarrow Mn^{+4}$ (bulk) + Mn^{+2} (solution), and oxidation–polymerization of pyrrole coupled with manganese reduction: $Mn^{+4} \rightarrow Mn^{+3}$. To avoid these two competitive processes and allow a better control of the reaction, we started from λ-MnO_2 and used lithium paratoluene sulfonate in water. In that case, the only reaction is the oxidative polymerization of pyrrole coupled with reduction of λ-MnO_2 and reintercalation of lithium ions, so that the amount of remaining λ-MnO_2 inversely scales with the amount of PPy coated (Fig. 4).

3.3. X-ray diffraction (XRD) analysis

Possible structure modifications of the starting spinel materials were investigated by powder X-ray diffraction and compared to XRD pattern of pure $LiMn_2O_4$ (cf. Fig. 5). It appears that the spinel XRD pattern is shifted to the one of pure delithiated λ-MnO_2 as the Py amount is increased in the polymerization bath, as evidenced by the shift of scattering angles to higher values, due to the decrease in the lattice parameter *a* when smaller Mn^{4+} ions replace Mn^{3+} cations. The surface modification by a PPy shell induces structural modifications of the core particles by changing the lattice parameter *a* and lowering the crystallinity. The decrease in lattice parameter is related to delithiation of the starting spinel and creation of the λ-MnO_2 phase. These results are confirming those of TGA. Conversely, when starting from λ-MnO_2, we observe a continuous shift of the Bragg peaks to the small angles, indicating a reduction of Mn^{4+} to Mn^{3+}, concomitant with lithium reintercalation.

3.4. Scanning electron microscopy (SEM)

SEM images of hybrid particles clearly demonstrate the presence of a polypyrrole skin covering $LiMn_2O_4$, whose aspect strongly differs from the one of $LiMn_2O_4$ crystals

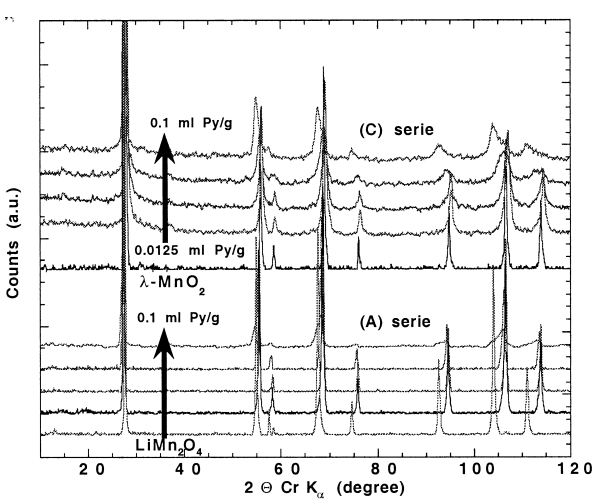

Fig. 5. Evolution of XRD patterns with the amount of Py used for $LiMn_2O_4$–PPy samples of series A and C.

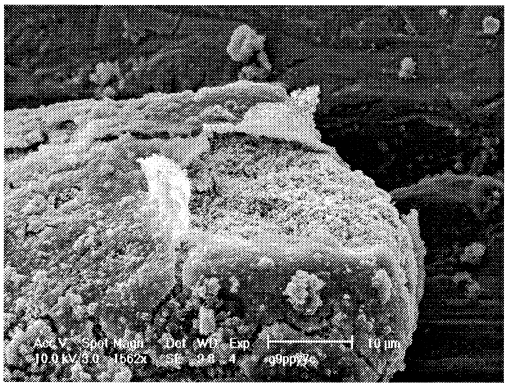

Fig. 6. SEM image of sample #0.05 A.

(Fig. 6). However, the adherence of PPy to the particles does not seem to be very strong, which certainly comes from the absence of covalent bonds at the organic–inorganic interface.

3.5. Electrochemical tests

Electrochemical tests of the hybrid material were performed at $C/10$ rate and room temperature for the measurements of capacities, and $1C$ or $C/2$ at 55°C for the investigation of cyclability in strenuous conditions. As one can see in Fig. 7, the general behaviour of the PPy-coated spinel was that of $LiMn_2O_4$ and not that of PPy.

This may be related to the fact that PPy is generally doped and undoped between 2 and 4 V vs. Li^+, Li whereas higher potentials are used when charging and discharging $LiMn_2O_4$ on the 4-V plateau, which may have a deleterious effect (oxidation) on the PPy coating. It may also be due to the low conjugation length of PPy as suggested by IR spectroscopy. Nevertheless, the PPy presence has a strong influence on the electrochemical behaviour of $LiMn_2O_4$, in terms of capacity and cyclability. In series A, The #0.1A sample could not be charged and discharged, and the best results (lowest capacity fading) were obtained at an intermediate PPy level (#0.0125A and #0.025A samples). How can we explain these results?

It seems that PPy is not governing the electrochemical behaviour, since the #0.0062A and #0.05A samples have almost the same capacities (corrected from the PPy amount) and the same capacity fading upon cycling, whereas their PPy content is totally different. It rather seems that the important parameter is the λ-MnO_2 content of the particles, which is the same in our example. Furthermore, in series A, the capacities at the beginning of cycling may be calculated from the λ-MnO_2 content determined from TGA analysis by using the following empirical relation:

$$C\left(\mathrm{mA\,h\,g^{-1}}\right) = 144(100 - \%\,\lambda\text{-}MnO_2)$$

where 114 mA h g^{-1} is the maximum practical capacity obtained with pure $LiMn_2O_4$ in the conditions of our experiments. As one can see in Fig. 8, the calculated capacities fit quite well with the experimental capacities of our composites. This clearly demonstrates that the λ-MnO_2 formed during the course of PPy polymerization is electrochemically inactive, which is quite surprising since λ-MnO_2 is known to reversibly intercalate Li ions. Furthermore, particles with the highest λ-MnO_2 content have the lowest capacity fading upon cycling. Thus we can conclude that this electrochemically inactive λ-MnO_2 acts like a passivation layer which protects the $LiMn_2O_4$ from capacity fading. Such an inactive form of 'λ-MnO_2' is not formed when the polymerization of pyrrole is incomplete (B series) or when the reaction is performed without the presence of protons (C series). Note that the samples of series C had a bad cyclability, which may have been caused by the increase in the specific surface area during the acid leaching step of synthesis. However, several sam-

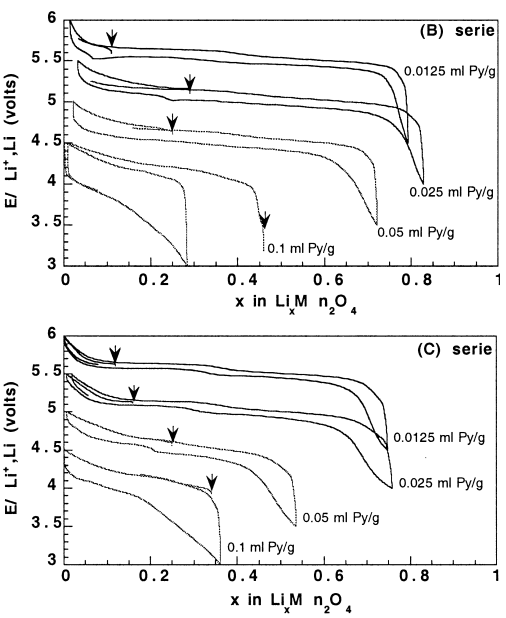

Fig. 7. Potential versus lithium intercalation degree at $C/10$ rate and 25°C for $LiMn_2O_4$–PPy samples of series B and C. Arrow = initial lithium content.

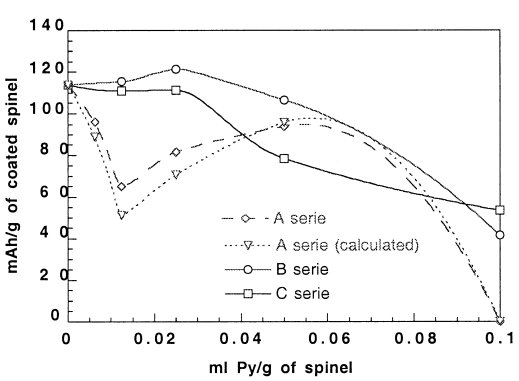

Fig. 8. Capacities as a function of initial amount of Py used for series A, B and C, and capacities calculated from λ-MnO_2 content for series A.

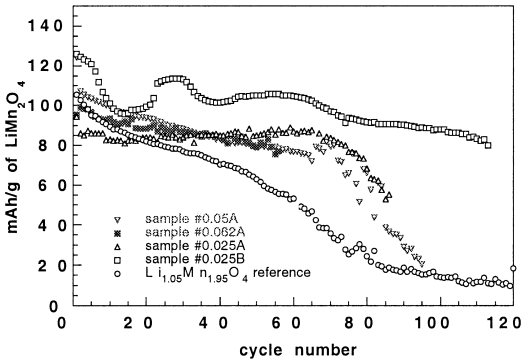

Fig. 9. Capacity fading with the number of cycles at $C/2$ rate and 55°C for several samples of series A and B.

ples of series A and B demonstrated an improvement in cyclability compared to pure $Li_{1.05}Mn_{1.95}O_4$ (Fig. 9).

4. Discussion

To account for all the results observed, we suggest a polymerization mechanism in two competitive steps that are the following:

(1) Dismutation of $LiMn_2O_4$ in acidic medium according to Hunter's reaction:

$$2LiMn_2O_4 \overset{H^+}{\rightarrow} 3\lambda\text{-}MnO_2 + Li_2O + MnO$$

(2) Reductive protonation of λ-MnO_2 coupled with oxidative polymerization of pyrrole:

$$\lambda\text{-}MnO_2 + H^+ + e^- \rightarrow H\text{-}\lambda\text{-}MnO_2$$

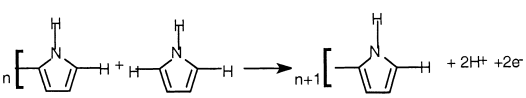

This mechanism is in agreement with all our experimental observations, e.g., (i) reddish coloration of the polymerization bath caused by the presence of MnO; (ii) delithiation of the starting spinel as observed on XRD patterns, TGA curves and first electrochemical cycles; (iii) loss of gravimetric capacity caused by the formation of partially electrochemically inactive H-λ-MnO_2.

5. Conclusions

There are two competitive reactions during the synthesis of $LiMn_2O_4$–PPy composites in acidic medium: (i) dismutation of Mn^{+3} species resulting in an increase in the Mn^{+4} content in the bulk material; (ii) reduction of Mn^{+4} in Mn^{+3} and reintercalation of lithium or protons coupled with the oxidation of pyrrole. Thus, the reaction products are very sensitive to experimental conditions, e.g., order of introducing the reactants, stirring or not, reaction time, etc.

Electrochemical cycling tests clearly indicated that PPy itself had no protective effect on the capacity fading of $LiMn_2O_4$ at 55°C. However, at low PPy contents, several samples had a higher capacity and an improved cyclability. It rather seems that the reaction of pyrrole with $LiMn_2O_4$ in acidic medium causes a surface modification of the spinel (manganese dissolution) which partially prevents the cathode from further capacity fading. Regarding the possible applications of such composites, the conductivity of the PPy coating could be improved by lowering the reaction temperature and increasing the reaction time, but the stability of PPy at high potentials remains questionable, and other polymers such as polythiophene could also be investigated for their higher stability towards oxidation.

References

[1] F.K. Shokoohi, P.C. Waren, S.J. Greaney, J.M. Tarascon, A.S. Gozdz, G.G. Amatucci, The 37th Power Sources Conference Proceedings, Cherry Hill, NJ, June 17–20, 1996.
[2] J.M. Tarascon, W.R. McKinnon, F. Coowar, T.N. Bowmer, G.G. Amatucci, D. Guyomard, J. Electrochem. Soc. 141 (1994) 1421.
[3] G.G. Amatucci, C.N. Schmutz, A. Blyr, C. Sigala, A.S. Gozdz, D. Larcher, J.M. Tarascon, J. Power Sources, in press.
[4] Y. Xia, M. Yoshio, J. Power Sources 66 (1997) 123–129.
[5] Y. Xia, Y. Zhou, M. Yoshio, J. Electrochem. Soc. 144 (8) (1997) 2593.
[6] Y. Xia, M. Yoshio, J. Electrochem. Soc. 127 (1996) 856.
[7] G. Amatucci, I. Plitz, T. Bowmer, Proceedings of 10th International Battery Materials Associate (IBA) Battery Materials Symposium, Tucson, AZ, 1996.
[8] G.G. Amatucci, A. Blyr, C. Sigala, P. Alfonse, J.-M. Tarascon, Solid State Ionics 104 (1997) 13–25.
[9] A.H. Gemeay, H. Nishiyama, S. Kuwabata, H. Yoneyama, J. Electrochem. Soc. 142 (12) (1995) 4191–4195.
[10] H. Yoneyama, Y. Shoji, K. Kawai, Chem. Lett. 1067 (1989) .
[11] M. Iseki, K. Saito, K. Kuhuara, A. Mizukami, Synth. Met. 40 (1991) 117–126.
[12] J.C. Hunter, J. Solid State Chem. 39 (1981) 142.
[13] D. Guyomard, J.M. Tarascon, Solid State Ionics 69 (1994) 222.
[14] Method of making an Electrolyte Activatable Lithium-Ion Rechargeable Battery Cell, US Patent 5,456,000.
[15] W. Liang, J. Lei, C.R. Martin, Synth. Met. 52 (1992) 227–239.
[16] J.R. Dahn, E.W. Fuller, M. Obrovac, U. von Sacken, Solid State Ionics 69 (1994) 265–270.